Mon. Not. R. Astron. Soc. **000**, 000–000 (0000) Printed 2 February 2008 (MN LATEX style file v2.2)

Formation of Kuiper-belt binaries through multiple chaotic scattering encounters with low-mass intruders

Sergey A. Astakhov,[1⋆] Ernestine A. Lee [2,3]† and David Farrelly[2]‡
[1] *John von Neumann Institute for Computing, Forschungszentrum Jülich, D-52425 Jülich, Germany*
[2] *Department of Chemistry and Biochemistry, Utah State University, Logan, UT 84322-0300, USA*
[3] *FivePrime Therapeutics, 951 Gateway Boulevard, South San Francisco, CA 94080, USA*

arXiv:astro-ph/0504060v1 4 Apr 2005

Submitted 2004 November 7; Accepted 2005 April 4

ABSTRACT
The discovery that many trans-neptunian objects exist in pairs, or binaries, is proving invaluable for shedding light on the formation, evolution and structure of the outer Solar system. Based on recent systematic searches it has been estimated that up to 10% of Kuiper-belt objects might be binaries. However, all examples discovered to-date are unusual, as compared to near-Earth and main-belt asteroid binaries, for their mass ratios of order unity and their large, eccentric orbits. In this article we propose a common dynamical origin for these compositional and orbital properties based on four-body simulations in the Hill approximation. Our calculations suggest that binaries are produced through the following chain of events: initially, long-lived quasi-bound binaries form by two bodies getting entangled in thin layers of dynamical chaos produced by solar tides within the Hill sphere. Next, energy transfer through gravitational scattering with a low-mass intruder nudges the binary into a nearby non-chaotic, stable zone of phase space. Finally, the binary hardens (loses energy) through a series of relatively gentle gravitational scattering encounters with further intruders. This produces binary orbits that are well fitted by Kepler ellipses. Dynamically, the overall process is strongly favored if the original quasi-bound binary contains comparable masses. We propose a simplified model of chaotic scattering to explain these results. Our findings suggest that the observed preference for roughly equal mass ratio binaries is probably a real effect; that is, it is not primarily due to an observational bias for widely separated, comparably bright objects. Nevertheless, we predict that a sizeable population of very unequal mass Kuiper-belt binaries is likely awaiting discovery.

Key words: celestial mechanics - methods: N-body simulations - minor planets, asteroids - Kuiper Belt - binaries: general - scattering

1 INTRODUCTION

Binary systems occupy a special place in astronomy. First and foremost they allow the determination of binary partner masses which, in the case of stars, proved critical in the early development of the mass-luminosity relation (Eddington 1924; Noll 2003). In fact, the majority of all stars seem to be members of gravitationally bound multiplets with most being members of binaries (Heggie & Hut 2003). The dynamics and energetics of star clusters, in particular, are strongly influenced by the presence of binaries. This is because the largest single contributor to the total mechanical energy of the cluster may be the internal energy (binding energy) of binaries (Hills 1975; Inagaki 1984; Janes 1991; Heggie & Hut 2003). Not surprisingly the dynamics of binary systems and their formation mechanism are a subject of continuing interest in stellar dynamics (Heggie 1975; Hills 1975, 1983a,b, 1990; Mikkola & Valtonen 1992; Mardling 1995a,b; Quinlan 1996; Heggie & Hut 2003).

Binaries are also relatively common in planetary physics; these include the Earth-Moon and Pluto-Charon systems (Christy & Harrington 1978; Canup & Asphaug 2001; Canup 2004, 2005) as well as a substantial number of asteroid binaries in the main belt. Asteroid binaries usually contain partners with mass ratios in the range $m_r \sim 10^{-3} - 10^{-4}$ where $m_r = m_2/m_1$ and m_1 and m_2 are the masses of the primary and secondary binary partners respectively. Objects with such asymmetric masses are most often thought of as "asteroids with satellites" (Merline et al. 2003) rather than as "binaries" although there exists no

⋆ E-mail: s.astakhov@fz-juelich.de; www.astakhov.newmail.ru
† E-mail: ernestine.lee@gmail.com
‡ E-mail: david.farrelly@gmail.com

Reference	**Mechanism**	**Notes**
Path 1 (Weidenschilling 2002)	Physical collision and subsequent accretion of two bodies inside Hill sphere of a third, larger Kuiper-belt object.	Depends on existence of approximately two orders of magnitude more massive bodies in the primordial Kuiper-belt than is currently accepted. At time of binary formation 99% of total mass of Kuiper-belt thought to be in much smaller bodies (Goldreich et al. 2002; Kenyon & Bromley 2004).
Path 2 (Goldreich et al. 2002)	Transitory binary formation inside Sun-binary Hill sphere. Capture and stabilization by dynamical friction.	Predicts primordial binary formation rate $\approx 3 \cdot 10^{-6}$ per year per large body. Assumes larger sea of small (< 10 km) bodies than gravitational instability theories predict (Funato et al. 2004). Predicts formation of multiplets.
Path 3 (Goldreich et al. 2002)	Transitory binary formation inside Sun-binary Hill sphere. Capture and stabilization by gravitational scattering with a single large intruder – L^3 mechanism.	Predicts primordial binary formation rate $\approx 3 \cdot 10^{-7}$ per year per large body. No explicit mechanism provided for gradual reduction in post-capture binary orbit semimajor axes.
Path 4 (Funato et al. 2004)	Initial production of asymmetric mass ratio "asteroid-like" binaries through physical collisions. Subsequent scattering encounters with large intruders then equalize mass ratio through exchange reactions.	Neglects solar tidal effects. Exclusively produces binaries with eccentricities $e > 0.8$. Effect of varying intruder mass not studied. Predicts future TNO binary discoveries will have roughly equal masses, large separations and high eccentricities.
Chaos-assisted capture (this article)	Transitory binary formation through chaos-assisted capture (Astakhov et al. 2003) inside Sun-binary Hill sphere. Subsequent stabilization through a sequence of gravitational scattering encounters with small intuders each having ca. $1-2\%$ of total binary mass.	Includes solar tidal effects. Predicts *ab initio* the formation of (i) binaries with moderate eccentricities $0.2 < e < 0.8$ and (ii) a preference for roughly equal mass binaries. Also predicts that future higher resolution surveys of the Kuiper-belt will discover populations of asymmetric mass binary TNOs. Mechanism suggests that binaries formed when the KB disk was dynamically cold, *i.e.,* prior to excitation and depletion of the Kuiper-belt (Duncan & Levison 1997; Gomes 2003; Morbidelli, Emel'yanenko & Levison 2004).

Table 1. Proposed Kuiper-belt binary formation mechanisms.

meaningful quantitative distinction between these definitions. The recent discovery of binary trans-neptunian objects (TNOs) is particularly significant because these objects allow for the direct determination of TNO masses thereby opening up an important window into the origin, evolution and current composition of the Kuiper-belt (KB) (Stewart 1997; Toth 1999; Luu & Jewitt 2002; Noll 2003; Gladman 2005). It is quite remarkable that recent systematic searches (Trujillo & Brown 2002; Noll 2003; Schaller & Brown 2003) seem to suggest that up to 10% of Kuiper-belt objects might exist as gravitationally bound pairs (Burns 2004).

Kuiper-belt binaries (KBBs) are notable for their unusual compositional and orbital properties as compared to main-belt asteroids: the most salient are (Noll 2003) (*i*) large mutual orbits, (*ii*) highly eccentric mutual orbits and (*iii*) mass ratios of order unity (Margot 2002; Veillet et al. 2002; Durda 2002; Weidenschilling 2002; Goldreich, Lithwick & Sari 2002; Noll 2003; Schaller & Brown 2003; Osip, Kern & Elliot 2003; Altenhoff, Bertoldi & Menten 2004; Funato et al. 2004; Burns 2004; Noll et al. 2004a,b; Takahashi & Ip 2004; Nazzario & Hyde 2005). However, in each case certain caveats apply (Noll 2003; Noll et al. 2004a,b). Firstly, by some measures KBB orbits are indeed large; *e.g.*, for main-belt asteroids with satellites the semimajor axis of the mutual orbit (a) is typically about an order of magnitude larger than the radius of the primary asteroid (r_A) whereas for KBBs $a/r_A \sim 50 - 500$ (Merline et al. 2003; Noll et al. 2004b). Curiously, however, if the semimajor axis is compared to the radius of the binary's Hill sphere (R_H) then

main-belt asteroid binaries and KBBs have rather similar semimajor axes, *i.e.*, expressed as a percentage $a/R_H \sim 2-5\%$ (Noll 2003; Noll et al. 2004b). Secondly, although KBB orbits are noticeably eccentric as compared to the almost circular orbits of main-belt asteroid binaries, recent observations suggest that extremely large eccentricities ($e > 0.8$) may be rarer than was initially thought (Noll 2003; Noll et al. 2004b). Finally, while the mass ratios of known KBBs are in the range $m_r \sim 0.1-1$ it is also possible that this result is at least partially due to an observational bias for well-separated, equally bright objects (Burns 2004). Nevertheless, the properties of KBBs are sufficiently striking to suggest that their formation mechanism differed considerably from that of main-belt or near-Earth asteroid binaries, which are thought to have been produced by physical collisions (Chauvineau, Farinella & Harris 1995; Xu et al. 1995; Durda et al. 2005).

Four different pathways (Weidenschilling 2002; Goldreich et al. 2002; Funato et al. 2004) – summarized in Table 1 – have been proposed to explain the formation and properties of KBBs which we will refer to as Paths 1 – 4: Path 1 involves physical collisions between two planetesimals within the Hill sphere of a larger Kuiper-belt object (Weidenschilling 2002). The two bodies then accrete and remain gravitationally bound as a single object to the larger body, thereby producing a binary. This mechanism assumes that binary objects are primordial; Similar to Weidenschilling's mechanism (Weidenschilling 2002) Paths 2 and 3 also proceed from the temporary gravitational capture of two objects within the three-body Hill sphere. Now, however, the large third body is the Sun (Goldreich et al. 2002). In both Paths 2 and 3 the initial stage of binary formation is the formation of a transitory binary which will eventually ionize unless stabilization occurs first. Two stabilization mechanisms have been proposed; in Path 2 stabilization results from dynamical friction through interactions with a sea of smaller (< 10 km) Kuiper-belt bodies. In Path 3 the transitory binary is stabilized by energy loss through gravitational scattering with a large third body – the L^3 channel. Both of these mechanisms emphasize the importance of the Sun-binary Hill sphere (Szebehely 1967; Murray & Dermott 1999).

A common feature of Paths 2 and 3 is that immediately before and after capture the binary partners are following an essentially three-body orbit. That is, solar perturbations or tides are important. Thus the orbits are periodic, quasi-periodic or chaotic (Lichtenberg & Lieberman 1992) and, in general, cannot be well described by orbital elements of the Kepler problem (Murray & Dermott 1999). However, actual KBBs follow orbits which can be well fitted by Kepler ellipses (Veillet et al. 2002; Noll 2003; Osip et al. 2003; Noll et al. 2004a,b), *i.e.*, solar tides are relatively unimportant and the orbits are approximately two-body in nature. Therefore, a mechanism for gradually transforming captured – and, therefore, bound – quasiperiodic three-body orbits into (almost) periodic two-body orbits is required. We term this general process "Keplerization" – *i.e.*, the gradual energy loss of three-body binary orbits to produce orbits that are essentially Kepler ellipses. As three-body orbits lose energy their semimajor axes undergo a steady reduction in size. In principle, Keplerization may occur directly during the capture process itself (*e.g.*, as posited to happen in L^3) or it can happen more gradually after the initial capture event through, *e.g.*, continued dynamical friction over extended timescales (Goldreich et al. 2002).

Path 4, proposed by Funato et al. (2004), involves exchange reactions (Heggie & Hut 2003) in which the smaller member of an already bound "asteroid-like" binary is displaced by a larger body during a three-body encounter. This mechanism is essentially a variant of binary star-intruder scattering (Hills 1975, 1983a,b, 1990; Hut & Bahcall 1990; Heggie & Hut 2003). In this mechanism solar tides are ignored and both the pre- and post-collision binary (if it survives) follow a two-body Keplerian ellipse.

While each of these four pathways is feasible, no consensus has yet emerged as to their relative importance or even whether a different mechanism altogether might have operated (Burns 2004). This is because each mechanism admits at least one potentially serious drawback. The first three paths are sensitive to assumptions about the size distributions of Kuiper-belt objects (Funato et al. 2004). Path 1 depends on the existence of more large bodies in the Kuiper-belt than seems to be consistent with observations (Goldreich et al. 2002; Funato et al. 2004); The basis of Path 2 is dynamical friction which, to be effective, requires a much larger sea of small bodies than is predicted by current theories of planetesimal formation (Goldreich & Ward 1973; Wetherhill & Stewart 1993; Rafikov 2003; Bernstein et al. 2004; Funato et al. 2004; Kenyon & Bromley 2004). Further, it is unclear how and why dynamical friction should select preferentially for roughly equal mass ratio binaries. This assumes, of course, that the apparent preference for mass ratios of order unity is not an observational artefact (Burns 2004).

The L^3 channel (Goldreich et al. 2002), Path 3, depends on relatively rare close encounters between three large objects and, based on the estimates of Goldreich et al. (2002), it is unclear if these occurred often enough to produce the current population of KBBs. In this regard it is interesting to note that recent calculations suggest that, if the Kuiper-belt lost its mass through collisional grinding, then an order of magnitude more binaries were likely present in the primordial Kuiper-belt than has otherwise been thought (Petit & Mousis 2004). This illustrates that the number and size distributions of primordial KB objects might be subject to revision (Stern 2002; Bernstein et al. 2004; Kenyon & Bromley 2004; Petit & Mousis 2004; Elliot et al. 2005). A second drawback to Path 3 is that, as originally proposed, it provides no explicit mechanism – beyond possible post-encounter dynamical friction – for producing the approximately two-body Keplerian binary orbits which are actually observed (Veillet et al. 2002; Noll 2003; Schaller & Brown 2003; Osip et al. 2003; Noll et al. 2004a,b). It is unlikely, as our simulations confirm, that a single collision between a quasi-bound binary (*i.e.,* one that is following a three-body Hill trajectory) and a massive intruder will result in a two-body Keplerian binary orbit. Finally, Path 4 leads almost exclusively to binary eccentricities $e \geqslant 0.8$ and very large semimajor axes which may approach R_H itself (Funato et al. 2004). However, moderate eccentricities, in the range $0.25 \leqslant e \leqslant 0.82$, and semimajor axes that are only a few percent of R_H seem to be the rule (Noll 2003; Osip et al. 2003; Noll et al. 2004a,b).

In the model described herein the first step is the

formation of long-lived quasi-bound binaries through the recently proposed mechanism of chaos-assisted capture (CAC, Astakhov et al. 2003; Astakhov & Farrelly 2004; Trimble & Aschwanden 2003) in the Hill approximation (Szebehely 1967; Hénon & Petit 1986; Murray & Dermott 1999; Heggie & Hut 2003). In CAC particles become temporarily caught-up in thin chaotic layers within the Hill sphere of, in this case, the Sun-binary system. These chaotic layers, which separate regular from asymptotically hyperbolic (scattering) orbits, are the result of the perturbation of the Sun on the motion of the two bodies making up the binary. Because the orbits are chaotic any quasi-bound (transitory) binary which is formed will eventually break apart. However, the lifetimes of these quasi-bound objects can be sufficiently long that, in the interim, stabilization can occur. Since the chaotic layers in the Hill problem (Simó & Stuchi 2000; Astakhov et al. 2003; Astakhov & Farrelly 2004) lie adjacent to regular Kolmogorov-Arnold-Moser (KAM, Zaslavsky 1985; Lichtenberg & Lieberman 1992) regions, then, in principle, even relatively weak perturbations can switch the binary into such KAM regions and thereby lead to permanent capture.

Of course, the precise nature of the stabilization mechanism is the crux of the matter. We propose that capture and subsequent hardening of three-body Hill orbits (*i.e.,* Keplerization) (Hills 1975, 1983a,b, 1990; Quinlan 1996; Heggie & Hut 2003) proceed through chaotic gravitational scattering encounters with low-mass intruders which happen to transit the Hill sphere. Once a binary has been captured initially then further encounters with intruders are probable – about once every 3,000-10,000 years (Weidenschilling 2002) – and this can eventually produce binaries whose mutual orbits are Kepler ellipses. Empirically we find that the process is most efficient for equal mass binaries and relatively low-mass intruders having $\sim 2\%$ or less of the total binary mass. Incidentally, we argue that CAC is also the dynamical basis of the twin mechanisms proposed empirically by Goldreich et al. (2002).

To model the statistics of capture we compute capture probabilities in four-body (Sun, binary, intruder) Monte Carlo scattering simulations for various binary mass ratios in the Hill approximation (Scheeres 1998). Our simulations reveal a clear preference for equal mass binaries to survive multiple subsequent encounters as they harden through intruder scattering.

The paper is organized as follows; Section 2 introduces the equations of motion for the three- and four-body problem in the Hill approximation and provides a brief overview of how chaos can assist capture into stable three-body orbits (Astakhov et al. 2003; Astakhov & Farrelly 2004). Monte Carlo simulations in the four-body Hill approximation (Scheeres 1998) are described in Sec. 3. A simplified (reduced dimensionality) model of chaotic low-mass intruder scattering is introduced in Sec. 4 to explain our results. To study the dynamics in this model we employ the Fast Lyapunov Indicator for several mass ratio and binary eccentricity combinations. A more detailed comparison with the other formation models summarized in Table 1 is made in Sec. 5. Conclusions are in Sec. 6.

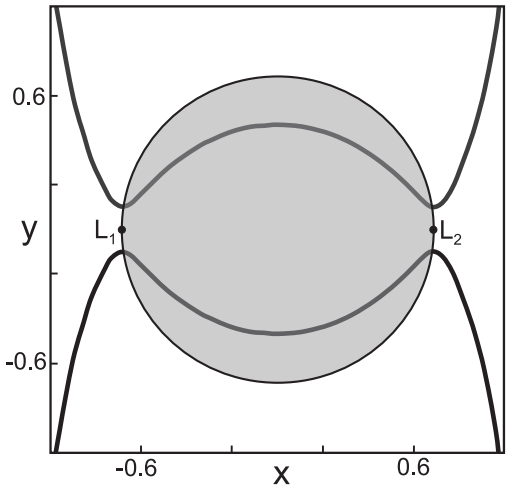

Figure 1. Typical level curves of the zero-velocity surface together with the Lagrange points L_1 and L_2 for the three-body Hill problem in the planar limit (Murray & Dermott 1999). The circle shaded grey shows the location of the Hill sphere. The Lagrange points demark the gateways into the capture zone. All units are scaled Hill units.

2 EQUATIONS OF MOTION IN THE THREE-BODY AND FOUR-BODY HILL PROBLEMS

In our model the initial stages of binary formation involve temporary capture within the Sun-binary Hill sphere through two particles getting entangled in chaotic regions of phase space, *i.e.*, chaos-assisted capture (Astakhov et al. 2003; Astakhov & Farrelly 2004). This process is well described in the three-body Hill approximation.

2.1 Three-body Hill problem

The three-body vector equations of motion in the Hill approximation are given by (Szebehely 1967; Hénon & Petit 1986; Murray & Dermott 1999; Scheeres 1998)

$$\ddot{\boldsymbol{\rho}} + \boldsymbol{\Omega} \times [2\dot{\boldsymbol{\rho}} + \boldsymbol{\Omega} \times \boldsymbol{\rho}] = -\boldsymbol{\rho} + 3\mathbf{a}(\mathbf{a} \cdot \boldsymbol{\rho}) - \frac{\boldsymbol{\rho}}{|\boldsymbol{\rho}|^3} \tag{1}$$

Here $\boldsymbol{\rho} = \boldsymbol{\rho}_2 - \boldsymbol{\rho}_1$ is the relative distance between the binary members which have masses m_1 and m_2 and whose centre-of-mass is assumed to move along a circular orbit $\mathbf{a} = (1, 0, 0)$ around a larger body m_0 (the Sun). The coordinate system (x, y, z) is rotating with constant angular velocity $\boldsymbol{\Omega} = (0, 0, 1)$ which corresponds (in scaled units) to the mean motion of the binary centre of mass. In this coordinate system the centre-of-mass of the binary is located at the origin as is usual in the Hill problem (Murray & Dermott 1999).

Units and typical values of parameters are defined as follows with reference to 1998 WW_{31} (Veillet et al. 2002): $m_1 \sim 2 \cdot 10^{21} g$, $m_2 \sim 10^{21} g$; the semimajor axis of the primary orbit $a_b \sim 45 AU$ and of the mutual binary orbit $a \sim 22000$ km. The Hill sphere (see Fig. 1) occupies the region between the saddle points L_1 and L_2 of the Hill problem which we term the "capture zone" (Szebehely 1967; Scheeres 1998; Murray & Dermott 1999); The Hill radius $R_H = a_b \left(\frac{m_1+m_2}{3m_0}\right)^{1/3}$; in physical units: $R_H \sim 3 \cdot 10^5$km $\sim 25a$.

In scaled Hill units (Szebehely 1967; Murray & Dermott 1999) $R_H = (1/3)^{1/3}$ and the radii of the binary partners $r_A \sim 10^{-4}$.

2.2 Chaos-assisted capture in Hill's problem

In order for a transitory (quasi-bound) binary to form two bodies must come inside their mutual Hill sphere defined with respect to the Sun. The Lagrange saddle points L_1 and L_2 in Fig. 1 serve as gateways between the interior of the Hill sphere and heliocentric orbits. Figure 2a shows a typical chaotic binary orbit obtained by integrating Hill's equations (1) in two-dimensions. The orbit is trapped close to a periodic orbit for many periods before finally escaping from the Hill sphere (not shown). The accompanying Poincaré surface of section (SOS) in Fig. 2b shows that the orbit is actually trapped in a chaotic layer separating a regular KAM island from a large region of hyperbolic scattering. Note that the orbits shown in Fig. 2 correspond to the mutual Hill orbit of the two binary partners and are independent of the particular mass ratio of the binary partners (Hénon & Petit 1986; Murray & Dermott 1999).

Examination of Poincaré surfaces of section in the Hill problem (Simó & Stuchi 2000) – or, equivalently, the circular restricted three-body problem (CRTBP) for small masses (Astakhov et al. 2003) – reveals that, at energies above the Lagrange saddle points L_1 and L_2 all phase space is divided into three parts, one of which regular KAM orbits inhabit, chaotic orbits another, the third consists of direct scattering orbits or, in other words, hyperbolic orbits. All these differ from each other in the behaviour of their orbits. The chaotic orbits separate the regular from the hyperbolic regions – see Fig. 2b. As energy is increased above the saddle points the chaotic regions consist of relatively thin layers of chaos which cling to the progressively shrinking KAM tori (Simó & Stuchi 2000; Astakhov et al. 2003; Astakhov & Farrelly 2004). Because incoming orbits cannot penetrate the regular KAM tori in 2-dimensions (2D) and only exponentially slowly in 3D (Lichtenberg & Lieberman 1992; Astakhov et al. 2003), orbits entering the Hill sphere from heliocentric orbits must either enter chaotic layers or scatter out of the Hill sphere essentially immediately.

Binaries corresponding to chaotic orbits lying close to KAM tori can themselves follow almost regular orbits for very long times as shown in Fig. 2a. In the presence of a source of dissipation or of other perturbations these orbits can easily be switched into the nearby, but otherwise impenetrable, KAM regions.

It is remarkable that capture can occur if the binary decreases or increases its energy during the encounter. This can happen because the topologies of stable KAM islands are, in general, a non-linear function of energy as is illustrated for four selected energies in Fig. 2c. That is, if a perturbation causes a chaotic orbit to increase or decrease its energy suddenly it may, in either event, find itself captured in a nearby regular part of phase space. Alternatively, such perturbations, though small, may cause the quasi-bound binary to break up more quickly if the size of the chaotic layer is suddenly reduced in favour of scattering regions.

Possible energy loss mechanisms which can stabilize transitory binaries include physical collisions (Weidenschilling 2002), gravitational scattering with other bodies and dynamical friction (Goldreich et al. 2002). Ruling out physical collisions and dynamical friction for reasons already described leaves gravitational scattering with "intruder" objects which enter the binary Hill sphere. The efficiency of this process depends critically on the intruder mass. For example, we find that the delicate chaotic binary orbits tend to be catastrophically destabilized by large intruders as, *e.g.*, in the L^3 mechanism (Goldreich et al. 2002). Further, as Fig. 2 shows, the orbits of transitory binaries can be a very large fraction of the Hill radius whereas actual binary orbits are typically only a few percent of R_H. Any KBB production mechanism must, therefore, explain how these large initial orbits are transmogrified into compact, Keplerian orbits. It is unlikely (as our simulations will show) that a single scattering encounter would propel the binary into such a final state directly. Rather, we propose that a series of gentle scattering encounters with low-mass intruders is necessary to capture and finally produce Keplerian orbits. Gentle stabilization by low mass intruder scattering is possible because only a weak perturbation is needed to drive long-lived chaotic orbits into adjacent regular regions of phase space.

2.3 Four-body Hill problem

The simulation of intruder scattering is facilitated by studying intruder scattering in the four-body (Sun, binary, intruder) Hill approximation (Scheeres 1998; Brasser 2002; Scheeres & Bellerose 2005). This approximation is appropriate given the mass ratios involved and the low to moderate eccentricities of typical KBB centre-of-mass orbits around the Sun.

The generalization of the Hill problem (Szebehely 1967; Hénon & Petit 1986; Murray & Dermott 1999) to the case where three small bodies, with a mutual centre-of-mass, $\mathbf{R}_c$, orbit a much larger fourth body (the Sun, $m_0 = 1$) on a near circular orbit (*e.g.*, three Kuiper-belt objects within their mutual Hill sphere) is due to Scheeres (1998). The total mass of the three bodies is defined by

$$\mu = \sum_{j=1}^{3} m_j \ll 1 \tag{2}$$

where $\mathbf{R}_c \approx \mathbf{a} = (1, 0, 0)$ defines the motion of the three-body centre-of-mass along an almost circular orbit which defines the rotating frame. The vector equations of motion are (Scheeres 1998)

$$\ddot{\boldsymbol{\rho}} + \boldsymbol{\Omega} \times [2\dot{\boldsymbol{\rho}} + \boldsymbol{\Omega} \times \boldsymbol{\rho}] = -\boldsymbol{\rho} + 3\mathbf{a}(\mathbf{a} \cdot \boldsymbol{\rho}) - (\alpha_1 + \alpha_2)\frac{\boldsymbol{\rho}}{|\boldsymbol{\rho}|^3} +$$

$$\alpha_3 \left(\frac{\boldsymbol{\rho}_3 - \boldsymbol{\rho}_2}{|\boldsymbol{\rho}_3 - \boldsymbol{\rho}_2|^3} - \frac{\boldsymbol{\rho}_3 - \boldsymbol{\rho}_1}{|\boldsymbol{\rho}_3 - \boldsymbol{\rho}_1|^3} \right) \tag{3}$$

$$\ddot{\boldsymbol{\rho}}_3 + \boldsymbol{\Omega} \times [2\dot{\boldsymbol{\rho}}_3 + \boldsymbol{\Omega} \times \boldsymbol{\rho}_3] = -\boldsymbol{\rho}_3 + 3\mathbf{a}(\mathbf{a} \cdot \boldsymbol{\rho}_3) -$$

$$\alpha_1 \frac{\boldsymbol{\rho}_3 - \boldsymbol{\rho}_1}{|\boldsymbol{\rho}_3 - \boldsymbol{\rho}_1|^3} - \alpha_2 \frac{\boldsymbol{\rho}_3 - \boldsymbol{\rho}_2}{|\boldsymbol{\rho}_3 - \boldsymbol{\rho}_2|^3} \tag{4}$$

Here $\boldsymbol{\rho}_3$ is the coordinate of the third intruder body, m_3, and $m_j = \mu\alpha_j$ where

$$\sum_{j=1}^{3} \alpha_j = 1. \tag{5}$$

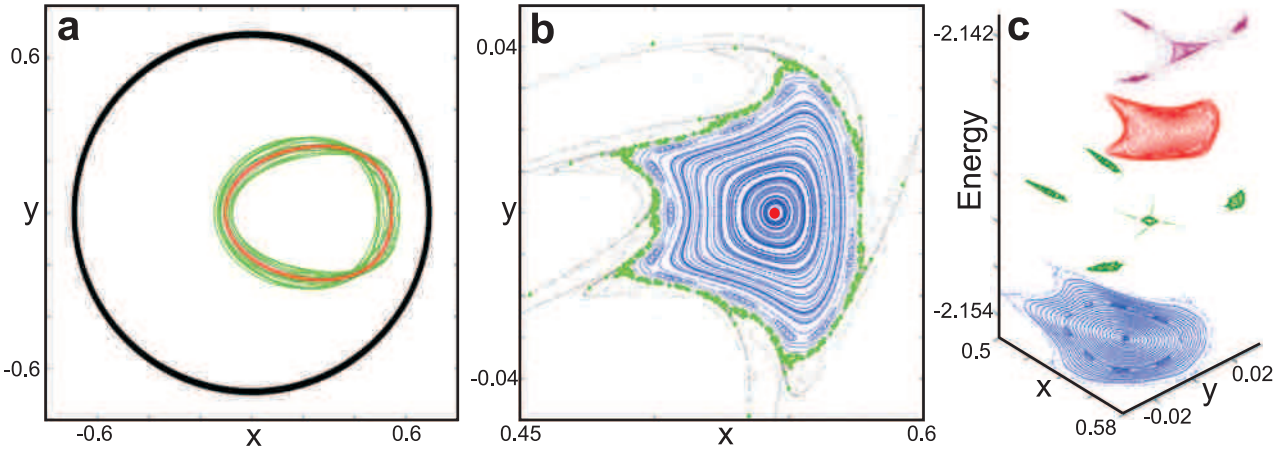

Figure 2. Non-linear dynamics of transitory binary formation in Hill's three-body problem. Panel (a) shows a quasi-bound (chaotic) binary centre-of-mass orbit (green) temporarily trapped close to a periodic orbit (red) which lies at the centre of a stable KAM island. This trajectory eventually escapes from the Sun-binary Hill sphere (large black circle). Panel (b) is a composite showing the colour coded SOS ($x-y$ hyperplane defined such that the momentum $p_x = 0$ and the velocity $\frac{dy}{dt} > 0$) for the trajectories in panel (a) and also several nearby chaotic (grey) and quasi-periodic (blue) orbits. Panel (c) shows the non-linear evolution of the size and shape of the KAM island in (b) with energy at four selected energy values. Distances and energies are in scaled Hill units.

Equations (3) and (4) contain the coordinates $\boldsymbol{\rho}_1, \boldsymbol{\rho}_2$ explicitly; this is purely for compactness of notation and, in practice, they are eliminated using the centre-of-mass relation

$$\sum_{j=1}^{3} \alpha_j \boldsymbol{\rho}_j = 0. \tag{6}$$

When $m_3 = 0$ equation (3) reduces to the three-body Hill problem (1) (Szebehely 1967; Murray & Dermott 1999) and becomes uncoupled from equation (4). Equation (4) is then a variant of the restricted Hill four-body problem (Scheeres 1998) and depends explicitly on the solution $\boldsymbol{\rho}(t)$ which may be periodic, quasi-periodic, or chaotic (Lichtenberg & Lieberman 1992; Astakhov et al. 2003). These solutions are actually particular trajectories for the three-body Hill problem.

To model the statistics of capture immediately after transitory binary formation we computed capture probabilities in four-body Monte Carlo scattering simulations as described in the next section.

3 MONTE CARLO SCATTERING SIMULATIONS

We are primarily interested in binary-intruder scattering, with intruders approaching from infinity. Therefore we assume that the transitory binary is initially following a chaotic, but long-lived *three-body* Hill orbit.

Because our Monte Carlo scattering simulations involve chaotic binary orbits they differ in essential respects from previous simulations; to our knowledge all previous simulations have dealt with intruder scattering from bound binaries which follow circular or elliptical two-body Keplerian orbits (Hills 1975, 1983a,b, 1990; Hut & Bahcall 1990; Heggie & Hut 2003; Funato et al. 2004). Therefore it is necessary to explain our procedure in detail.

In any energy range for which chaotic layers exist it is possible to find an infinite number of initial conditions corresponding to different quasi-bound, three-body binary orbits (Lichtenberg & Lieberman 1992). This is illustrated in Fig. 2c; it is apparent that a swath of chaotic orbits over the energy range shown will not only have a range of lifetimes but their dynamics will depend sensitively on their particular initial conditions and energy. Since we are interested in the probability of capture from chaotic zones into stable KAM zones it is, therefore, necessary to study an *ensemble* of such orbits rather than a single example. That is, the capture probability of interest is not simply the probability of any given orbit being captured; it must also measure the density of "capturable" orbits inhabiting the chaotic zones.

3.1 Methods

The procedure we have developed is as follows:

(i) Initially a cohort of 170 different quasi-bound chaotic binary orbit initial conditions was harvested by integrating eq. (1) using a Bulirsch-Stoer method (Press et al. 1999; Aarseth 2003). Initial conditions were chosen randomly inside the three-body (Sun-binary) Hill sphere for randomly chosen negative energies lying above the (three-body Hill) Lagrange saddle points and in the energy range $-2.15 < E < -2.0$. If an orbit remained inside the Hill sphere for a time $T_1 < T_H < T_2$ then its initial conditions were stored. We refer to T_H as the orbit's "natural" Hill lifetime. In scaled units we chose $T_1 = 15$ (~ 600 years) and $T_2 = 50$. While much longer (and shorter) living orbits are possible selected integrations for such orbits produce comparable results. This procedure guarantees that all orbits in the cohort are chaotic since, absent perturbations, they all eventually exit the Hill sphere.

(ii) Equations (3) and (4) were integrated for various values of m_r and m_3 using the stored initial conditions for the binary, but rescaled to the actual values of m_1 and m_2 used. Thus, the same cohort of three-body quasi-bound Hill orbits was used for all mass ratios.

(iii) Intruder particles were fired at each binary orbit with the phase of the binary chosen randomly. For each binary orbit 5000 intruders were sent in and, each time, it was recorded whether the binary was stabilized or not. For each binary orbit this produces a capture probability, *i.e.*, the fraction of the 5000 intruders that lead to stabilization in a single encounter with a binary.

(iv) Intruders were started isotropically with uniformly chosen random positions on a sphere of radius R_H, with uniform random velocities $|v| \leqslant 5v_H$ where v_H is the Hill velocity (Goldreich et al. 2002; Funato et al. 2004; Goldreich, Lithwick & Sari 2004)

$$v_H \sim \Omega R_H, \tag{7}$$

with Ω being the orbital frequency of the third body around the binary at distance R_H.

(v) In order to choose the phase of the binary randomly intruder integrations were started at randomly chosen times $t \in (0, T_H)$ along the binary orbit. In practice this has the effect of sending the intruder towards the binary at different relative configurations of the binary partners in phase space.

(vi) The integrations proceeded until either the binary broke up or it survived for a time $t = 10\ T_H$ at which point it was considered captured. After the intruder escaped from a sphere of radius $3R_H$ the integrations for the binary continued assuming $m_3 = 0$, *i.e.*, the usual three-body Hill equations (1) were used.

(vii) At the end of the integration each captured binary and its intruder were back integrated in time to ensure that the binary (in the four-body integration) broke up in the past. This helps protect against accidentally starting the binary-intruder trinary in already bound regions of phase space.

(viii) Integrations were stopped if particles came within a distance $r_A = 10^{-4}$ of each other.

(ix) These simulations were repeated ten times so as to be able to compute variances (error bars) for the capture probabilities. Each time a different random number seed was used to guarantee that the simulations were independent. Thus, *e.g.*, Orbit 1 may end up with capture probability 0.4 ± 0.02, Orbit 2, 0.23 ± 0.018, and so on.

(x) Orbits in the cohort were then binned according to their assigned capture probabilities. This produced histograms showing the number-density of orbits in the cohort having capture probabilities in the various specified intervals. Mainly the error bars were used (a) to establish that the calculations had converged and (b) to decide on a reasonable granularity for the probability bins.

(xi) The actual number of binary orbits included in the cohort was chosen so as to provide acceptable convergence given available computational resources. Convergence was judged acceptable when variances in capture probabilities were on the order of a few percent or less.

3.2 Single intruder scattering

In these simulations, each binary orbit in the cohort ends up with a capture probability and an error bar (of the order of a few percent) attached to it. However, for different mass ratios the same binary orbit in the cohort will, in general, have different capture probabilities and error bars. Figure 3

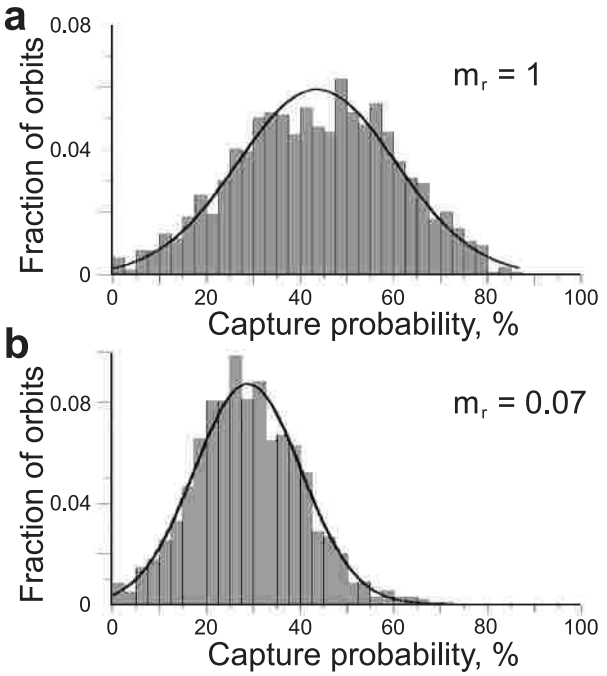

Figure 3. Fraction of binary orbits (number-density distributions) binned according to their individual capture probabilities as described in the text with $\alpha_3 = 0.025$; Mass ratios are (a) $\alpha_1 = \alpha_2$ and (b) $\alpha_1 = 14\alpha_2$ (b). Smooth curves are best fits to normal distributions. The same set of 170 chaotic Hill orbits in three-body centre-of-mass coordinates, appropriately rescaled, was used in both cases. The binary was considered captured only if the original binary partners remained bound to each other, *i.e.*, exchange reactions were ignored. In 98.5% of cases the average capture probability for any given Hill orbit was higher for equal mass binaries.

presents histograms showing the fraction of captured orbits binned according to their individual capture probabililities for two typical mass ratios. We tested that these histograms are robust to the actual number of binary orbits included in our cohort – *e.g.*, if 85 rather than 170 orbits are used the shapes of the histograms are essentially identical to those in Fig. 3. The width of the bins is roughly commensurate with the average width of the error bars.

The distributions in Fig. 3 clearly indicate that the fraction of binary orbits peaks at a significantly higher capture probability for equal mass ratio binaries than for unequal mass ratio binaries. This translates into a higher probability for capture in the equal mass case. Recall that the actual binary orbits used in both cases are identical. Since the cohort of binary orbits used is the same, and the intruder masses and initial conditions are also the same, then the difference in the distributions is due entirely to the different binary mass ratios employed. In fact the only parameter that was varied between the simulations shown in Fig. 3 was the mass ratio.

We also compared individual capture probabilities orbit for orbit and found that in 98.5% of cases the average capture probability for any given Hill orbit was higher in the equal mass simulation. Thus, at any fixed Hill radius (*i.e.*, the same total binary mass) a clear preference for the capture of same-sized binary partners is apparent. For comparison, the mass ratios m_r of the four best

characterized KBBs are ~ 0.57 (1998 WW_{31}, Veillet et al. 2002), ~ 0.56 ((66652) 1999 RZ_{253}, Noll et al. 2004a), ~ 0.55 ((58534) 1997 CQ_{29}, Noll et al. 2004b) and ~ 0.34 ((88611) 2001 QT_{297}, Osip et al. 2003). These are significantly larger than the mass ratios of main-belt binaries for which, as noted, $m_r \sim 10^{-3} - 10^{-4}$ (Merline et al. 2003).

The calculations for Fig. 3 took ~ 1 month using all nodes on a 32-node Beowulf cluster. Interestingly the mass effect manifested itself quite directly in that the simulations for Fig. 3b finished about a week earlier than those for Fig. 3a. This is because of the additional tests and integrations that needed to be performed to verify that an orbit had been captured permanently.

3.3 Multiple intruder scattering

The probabilities in Fig. 3 are for permanently capturing already-formed quasi-bound binaries through a *single* intruder scattering event. However, the overall probability of binary formation depends too on the probability of forming quasi-bound binaries in the first place. Because Hill's equations (1) are parameter free (after rescaling, Murray & Dermott 1999) once two objects come within their mutual Hill sphere the probability of chaos-assisted quasi-binary formation becomes independent of their relative masses. Nevertheless, the entry rate of bodies into each other's Hill sphere – and thus the overall capture probability – will depend on the actual masses and velocities of the objects involved. Uncertainties in the size and velocity distributions of contemporary and primordial Kuiper-belt objects means, however, that estimating Hill sphere entry rates is an open problem but one whose resolution should be aided by the discovery and characterization of further KBB objects (Petit & Mousis 2004; Bernstein et al. 2004; Kenyon & Bromley 2004; Noll et al. 2004b). Despite these uncertainties the mass effect is expected to persist because it is progressively enhanced by later scattering events.

After its initial capture through a single scattering encounter with an intruder a binary is, typically, following a very large three-body orbit with a semimajor axis similar in size to that of the periodic orbit illustrated in Fig. 2a. That is, though now bound, the binary partners are still strongly influenced by solar tides. In this subsection we demonstrate that essentially Keplerian two-body orbits can be produced through a series of subsequent scattering encounters with further small intruders.

That this is possible is demonstrated by the simulations underlying Fig. 4. In these simulations, for each mass ratio, a cohort of 1200 randomly chosen Hill binary orbits (in the energy range $-2.15 < E < -0.15$) was generated as described in the previous subsection. The scatter plot shows the final orbital elements of only those binaries out of the 1200 which survived $N_{enc} = 200$ successive encounters with intruders. Intruder initial conditions were generated as described previously. In this set of simulations an encounter was considered non-disruptive if the binary survived for $t > 50$ scaled Hill time units. The first intruder was sent in at a random point along the binary orbit during the orbit's Hill lifetime $t \in (0, T_H)$ (the binary orbit integration was itself started at $t = 0$). If the binary survived to $t = 50$ the next intruder was sent in. If the binary survived that event then the next intruder was sent in, and so on. Thus, intruders were spaced 50 time units apart. This was repeated until either the binary broke up or it survived N_{enc} such successive encounters.

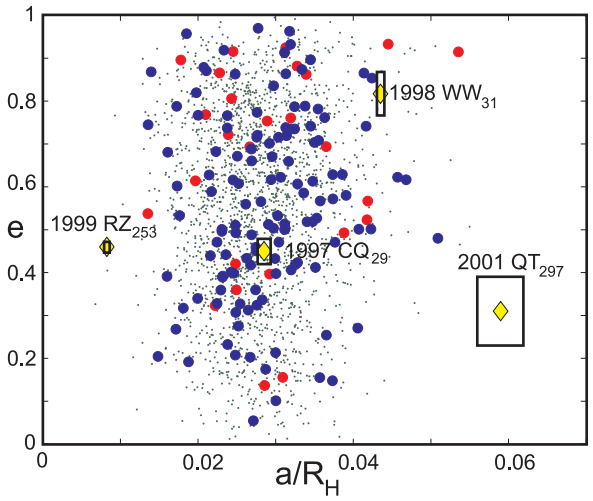

Figure 4. Distributions of orbital elements, eccentricity, e, and semimajor axis, a (scaled by the Hill radius R_H) after $N_{enc} = 200$ intruder scattering events per binary The figure combines results for twenty mass ratios: $m_r = \frac{\alpha_2}{\alpha_1} = 1$ (blue); $m_r = 0.05$ (red) and 18 intermediate values $0.1 \leqslant m_r \leqslant 0.95$ (green dots). Yellow diamonds show the locations of the four KBBs with known orbital elements (boxes are 1σ observational error bars) (Veillet et al. 2002; Osip et al. 2003; Noll et al. 2004a,b). For each mass ratio, 1200 different initial binaries were integrated to generate the figure. To accumulate statistics this simulation was repeated 60 times for the two extreme mass ratios. In each case 5000 (rather than 1200) initial binaries were used per mass ratio. After $N_{enc} = 200$ encounters binary survival probabilities were 0.103 ± 0.007 ($m_r = 1$) and 0.019 ± 0.002 ($m_r = 0.05$). The survival probability is defined as the fraction of the orginal 5000 binaries which remains bound after $N_{enc} = 200$.

In order to generate statistics it proved desirable to perform a much larger simulation than was actually used to produce Fig. 4. The capture probabilities and error bars given in the caption to Fig. 4 were obtained by repeating the simulations as described in 60 independent runs, in each case using an initial cohort of 5000 (instead of 1200) randomly chosen binary orbits.

Naturally, each of the binary-intruder encounters may individually be stabilizing or destabilizing. However, our simulations indicate that comparable mass binaries, especially, tend to survive multiple encounters as they harden through intruder scattering, thereby becoming more Keplerian; this is similar to the situation in low-mass intruder/binary-star scattering in which (depending on intruder velocity) orbits tend, on average, to harden (Hills 1975, 1983a,b, 1990; Heggie & Hut 2003). After $N_{enc} = 200$ intruder encounters Fig. 4 demonstrates that multiple scattering can produce KBBs with orbital elements comparable to those actually observed. Once a binary has been captured then further encounters with intruders are likely. We assume ~ 100 km-sized binary partners and intruders having masses $1 - 2\%$ of the total binary mass.Based on Weidenschilling's model we find that binary-intruder encounters will occur about once every 3,000-10,000 years (Weidenschilling 2002); Fig. 4 demonstrates that such encounters can eventually produce Keplerian orbits. Although the final orbits in Fig. 4 are

still strictly solutions to Hill's problem, their energy has been reduced sufficiently that, for all intents and purposes, they follow two-body Kepler ellipses, *i.e.,* the orbits are well described by Keplerian orbital elements (Murray & Dermott 1999).

Experimental simulations for multiple intruder encounters reveal that the main effect of increasing the number of encounters (N_{enc}) is to reduce the final value of the semimajor axis whereas the final eccentricity distributions were quite robust to N_{enc}. Thus we chose the single parameter $N_{enc} = 200$ heuristically so that orbits ended up roughly in the observed semimajor axis range of 1998 WW_{31}. Therefore, Fig. 4 represents a single parameter fit to the semimajor axis of one of the most well characterized KBBs. However, no special attempt was made to refine the fit.

Kuiper-belt binary semimajor axes – expressed as a fraction of the binary Hill radius – are generally comparable to those of asteroid binaries and Fig. 4 captures this finding. Figure 4 also reproduces the moderate eccentricities which seem to be a feature of actual KBBs (Noll et al. 2004b). This finding contrasts with the extremely large eccentricities ($e > 0.8$) produced exclusively in exchange reactions (Funato et al. 2004). Finally, Fig. 4 demonstrates that equal mass binaries have significantly higher survival probabilities than asymmetric mass binaries after multiple intruder encounters.

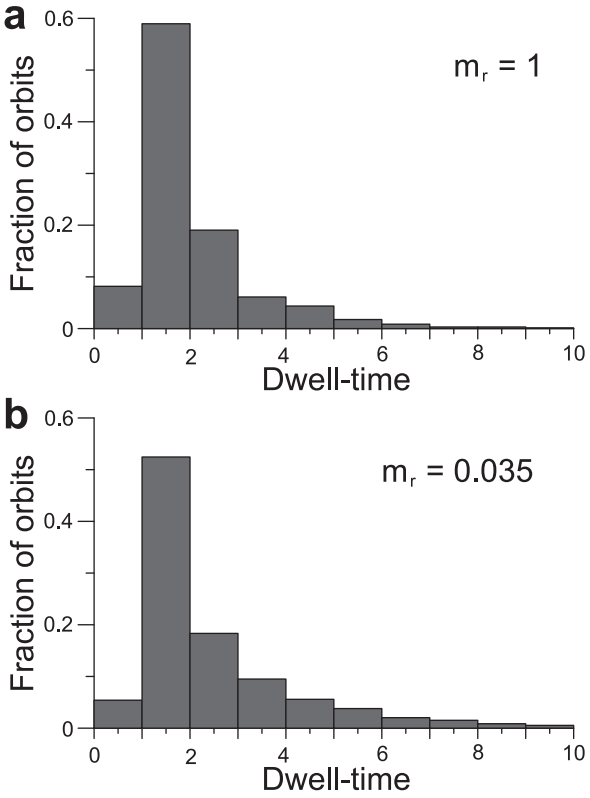

Figure 5. Dwell-time distributions for intruder scattering for (a) $m_r = 1$ and (b) $m_r = 0.035$. For each of the two mass ratios shown 5000 low-mass intruder scattering events were simulated as described in Sec. 3. The histograms show densities of intruders in various dwell-time ranges. Some dwell-times $t > 10$ occur but these have been omitted from the figure for clarity. For the sake of comparison, in these simulations, a single chaotic binary orbit was used but the results are similar if different chaotic binary orbits are used. An identical series of intruders was used in both cases. The Hill lifetime of the binary orbit used is $T_H \approx 17$ in scaled units. Intruders are binned according to the time they remain within the Hill sphere – their dwell-time. Average dwell-times are (a) 2.1 and (b) 2.7 scaled time units.

4 REDUCED MODEL OF INTRUDER SCATTERING

The simulations described so far indicate that roughly equal mass binaries have a statistically significantly higher capture probability than binaries with small mass ratios. However, the origin of this effect is not directly apparent from the simulations. In this section we develop a reduced model of intruder scattering which provides an explanation of the mass effect discovered in the simulations. The origin of this effect is related to chaotic scattering of the intruder by the binary.

4.1 Chaotic scattering and dwell times

Chaotic scattering involves a complex and sensitive dependence of some "output variable" (*e.g.*, scattering angle, interplay- or dwell-time, etc.) on an "input variable" (*e.g.*, impact parameter). For example, scattering in the CRTBP has been demonstrated to be chaotic (Boyd & McMillan 1993; Benet et al. 1997; Macau & Caldas 2002; Nagler 2004); Benet et al. (1997) plotted scattering functions (output energy and trajectory length) as a function of impact parameter and found clear evidence of chaotic scattering. Similar results were found by Boyd & McMillan (1993) who demonstrated chaotic scattering in binary star – intruder scattering. However, the high dimensionality of the four-body problem, even in the Hill approximation, makes it difficult to study a single output variable as a function of a single input variable. Nevertheless, we performed a series of exploratory simulations in which the dwell-time of the intruder inside the Hill sphere was calculated as a function of binary mass ratio. The dwell-time is here defined to be the total time the intruder remains inside the Hill sphere in our Monte Carlo single-encounter scattering simulations.

Fig. 5 presents typical histograms of intruder dwell times for two mass ratios. The dwell-time distributions for the two cases differ in that for unequal masses the distribution has a longer tail corresponding to longer dwell-times. That is, the intruder has a greater chance of becoming caught up in a long-lived resonance (Heggie & Hut 2003) if the binary has very asymmetric mass partners. The average dwell times shown are quite typical and are fairly consistent between different binary orbits. The unequal mass case typically has an average dwell-time $\approx 20-30\%$ longer than that for equal masses depending on the actual mass ratio used and the particular binary orbit selected.

In an attempt to understand this result and how (or if) it relates to the differential stabilization of equal and unequal mass binaries we have developed a simplified model of intruder scattering. The main reason why we resort to studying a simplified problem is the difficulty in visualizing the dynamics and the structure of the 12-dimensional phase space in the full four-body Hill problem. We stress, however,

that, in the following, we are only *interpreting* the dynamics exhibited in the full problem using reduced dimensionality dynamics. None of the results obtained in the previous section rely on this analysis.

Empirically it seems likely that the origin of the mass effect in Figs. 3 and 4 can be traced to the observed difference in intruder dwell- or interplay-times (Shebalin & Tippens 1996). This is because the only consistent difference we were able to find between simulations which were otherwise identical, except for having different mass ratios, was in intruder dwell-time distributions. A similar effect has also been observed by Hills in simulations of star stellar-binary scattering (Hills 1975, 1983a,b, 1990). However, Hills took the binary orbits to be bound, two-body Keplerian orbits rather than chaotic three-body orbits; *i.e.*, Hills' work does not contain the equivalent of solar tides which, in our model, are essential for the formation of quasi-bound binaries in the first place.

The model we build has its foundations in the following observations;

(i) A separation in timescales exists between fast intruder scattering and the timescale of the mutual binary orbit. That is, chaos in the binary orbit caused by solar tides generally develops on a slower timescale than does the intruder scattering event.

(ii) The difference in dwell-times between equal and unequal mass binaries is greatest for small intruders.

(iii) If simulations are done using zero-mass intruders then, clearly, no binary stabilization can occur. Nevertheless, the intruder dwell-time effect persists. In this limit the problem reduces to the so-called restricted Hill four-body problem (RH4BP) (Scheeres 1998).

(iv) Experimental simulations reveal that the dwell-time effect in the RH4BP exists even if the binary follows an elliptical Keplerian orbit. These findings are based on extensive simulations in the four-body Hill problem and in several variants of the RH4BP in which different solutions for $\boldsymbol{\rho}(t)$ were used – see the discussion following equation (6).

(v) As the binary hardens then solar tides become relatively less important and the problem reduces to the elliptic restricted three-body problem (ERTBP) (Scheeres 1998).

4.2 The Elliptic Restricted Three-body Problem

Combining the observations in the previous subsection leads to the following set of assumptions: neglect solar tides, assume elliptical binary orbits and set the intruder mass to zero. After making these approximations the four-body Hill problem reduces to the elliptic restricted three-body problem (Scheeres 1998) for which the Hamiltonian is given by (Szebehely 1967; Llibre & Piñol 1990; Mikkola & Valtonen 1992; Astakhov & Farrelly 2004);

$$H_e = \frac{1}{2}((p_x + y)^2 + (p_y - x)^2 + {p_z}^2 + z^2) -$$

$$\left(\frac{1-\mu'}{\sqrt{(1+x)^2+y^2+z^2}} + \frac{\mu'}{\sqrt{x^2+y^2+z^2}} + \right.$$

$$\left. \frac{1}{2}(x^2+y^2+z^2) + (1-\mu')x + \frac{1}{2}(1-\mu') \right) \Big/ (1 + e\,\cos\,f). \quad (8)$$

Here the semimajor axis of the *mutual* binary orbit a has been scaled to unity; e is the eccentricity of the binary orbit and $\mu' = m_2/(m_1+m_2)$ or $m_r = \mu'/(1-\mu')$. The true anomaly of the binary mutual orbit f, *i.e.*, the angular position measured from the pericentre, is related to the physical time t through (Szebehely 1967)

$$\frac{df}{dt} = \frac{(1 + e\,\cos\,f)^2}{(1-e^2)^{3/2}}. \quad (9)$$

The CRTBP Hamiltonian (Astakhov et al. 2003)

$$H_c = \frac{1}{2}({p_x}^2 + {p_y}^2 + {p_z}^2) - (x\,p_y - y\,p_x) -$$

$$\frac{1-\mu'}{\sqrt{(1+x)^2+y^2+z^2}} - \frac{\mu'}{\sqrt{x^2+y^2+z^2}} -$$

$$(1-\mu')x - \frac{1}{2}(1-\mu') \quad (10)$$

is recovered when $e = 0$. The Hamiltonians (8) and (10) are defined in the rotating frame with the origin transformed to one of the primaries.

Note that, in the following, the eccentricity being referred to in the context of the ERTBP is the eccentricity of the *mutual* orbit of the binary partners and not the *heliocentric* eccentricity of the binary centre-of-mass. The binary centre-of-mass is still assumed to be following a circular heliocentric orbit.

It is important to keep in mind that, in the ERTBP, the two primaries are assumed to be following an elliptical (Keplerian) mutual orbit and, therefore, these bodies cannot ionize. In our simplified model the ERTBP primaries are actually the binary partners which are, in reality, following an unbound chaotic orbit. However, if the intruder dwell-time is sufficiently small then, *during the intruder scattering event itself*, neither the intruder nor the binary will sense the longer timescale chaos caused by solar perturbations on the binary orbit. In a sense this picture is similar to the Born-Oppenheimer approximation for molecules in which the slow nuclei appear almost frozen from the point of view of the much faster electrons (Karplus & Porter 1970). It should be emphasized that, even if the intruder does not sense that the binary orbit is chaotic, the perturbation the intruder induces on the binary can, nevertheless, influence the binary orbit's long time development. That is the intruder can stabilize, destabilize, or leave essentially unaffected the evolution of the binary mutual orbit.

The ERTBP will, therefore, only be a reasonable model if the timescale of the binary partner relative motion is much slower than that of binary-intruder scattering encounters. If this is the case then the four-body Hill problem can be approximately decomposed into two simpler three-body systems; Sun-binary and binary-intruder. In practice, we find that intruder dwell times – the time the intruder spends inside the Hill sphere – in the full four-body simulations are normally no more than a few percent of the Hill lifetime of the orbit (T_H, defined earlier) and so we expect that studying the reduced (ERTBP) dynamics will be useful as a proxy for the full problem.

Stated somewhat differently, we make the assumption that the relative approach velocity of the massive binary partners is quite small whereas hardening requires that the intruder approach in a hyperbolic flyby at a somewhat

larger relative velocity. While this might seem contradictory, equipartition of energy in a particle disk implies that the largest bodies will have the most circular coplanar orbits, while the smaller bodies - here the intruders - will be more eccentric and inclined. Thus the relative velocity of approach should indeed be larger for the small intruders (Goldreich et al. 2002; Wetherhill & Stewart 1993; Stewart & Ida 2000; Lewis & Stewart 2002; Ohtsuki et al. 2002; Goldreich et al. 2004).

Because the binary is actually following an unbound chaotic orbit it is easily disrupted. Even small intruders can, in principle, lead to early disruption of the binary (as compared to T_H, the binary lifetime in the absence of intruders). If, on the one hand, the intruder has a short dwell-time then it is in and out of the Hill sphere quickly and there is an opportunity for sudden energy transfer with minimal disruption of the binary. Granted, this energy transfer may destabilize the binary but, in the intruder velocity regime of interest, we find that, on average, this is not the case – again this result is quite similar to the findings of Hills (Hills 1975, 1983a,b, 1990). Note especially that ionization of the binary is possible – though not necessarily equally likely – for small as well as large intruders. This situation should be contrasted with the case of already bound (Keplerian) binaries when, in general, a comparably massive intruder may be needed to produce complete or "democratic" ionization (Heggie & Hut 2003).

On the other hand if the intruder gets trapped in a relatively long-living resonance with the primaries then there exists a greater opportunity for disruption since the perturbation to the binary orbit is being applied for longer. That is, if the intruder gets caught up in a sticky chaotic layer its stay within the Hill sphere will be extended (in a resonance) as compared to if it had entered an asymptotically hyperbolic regime. While the lifetime of the resonance may still be much shorter than T_H it will be significantly longer than the dwell time of an intruder undergoing hyperbolic scattering. Such resonances have three main decay channels (Hills 1983b; Heggie & Hut 2003); (i) complete ionization, (ii) expulsion of the intruder and (iii) expulsion of one of the original binary partners (exchange). While channel (ii) is the most likely of the three for small intruders, channels (i) and (iii) can also occur because the binary orbit is not bound. Thus, as compared to sudden scattering, resonances (in the sense of long-lived trinary complexes (Heggie & Hut 2003)) tend, on average, to reduce the capture probability.

In view of the foregoing we suggest that the relative sizes of the *chaotic* regions as compared to the *hyperbolic* regions will correlate directly with the intruder's dwell-time. We argue that the relative sizes of these regions should, therefore, also correlate to capture probabilities. Chaos delays the intruder within the Hill sphere and so amplifies the effect of the intruder on the binary orbit. Repeated interactions – and energy transfer – between the binary and the intruder tend to destabilize the fragile binary orbit. Importantly, we are here comparing relative rather than absolute propensities for stabilization. Not all fast encounters are stabilizing nor do all resonances cause the binary to decay.

Thus, what requires examination is the relative size of *chaotic* versus *hyperbolic* regimes for various mass ratio/eccentricity combinations. The value of the ERTBP limit of the four-body Hill problem is that it allows one to visualize phase space directly; in this case using the Fast Lyapunov Indicator (FLI) as will now be described (Froeschlé, Guzzo & Lega 2000; Astakhov & Farrelly 2004).

4.3 Fast Lyapunov Indicator

The FLI is useful for mapping chaotic and regular regions of phase space when Poincaré SOS cannot readily be computed (Froeschlé et al. 2000; Pilat-Lohinger, Funk & Dvorak 2003; Astakhov & Farrelly 2004). Given an n-dimensional continuous-time dynamical system,

$$d\mathbf{x}/dt = \mathbf{F}(\mathbf{x}, t), \mathbf{x} = (x_1, x_2, ..., x_n), \tag{11}$$

the Fast Lyapunov Indicator is defined as (Froeschlé et al. 2000)

$$FLI(\mathbf{x}(0), \mathbf{v}(0), t) = \ln |\mathbf{v}(t)|, \tag{12}$$

where $\mathbf{v}$(t) is a solution of the system of variational equations (Tancredi, Sánchez & Roig 2001)

$$\frac{d\mathbf{v}}{dt} = \left(\frac{\partial \mathbf{F}}{\partial \mathbf{x}}\right)\mathbf{v}. \tag{13}$$

Regularization (Stiefel & Scheifele 1971; Aarseth 2003) was used to integrate equations (11) and (13).

4.3.1 Choice of initial conditions and energies in FLI maps

To analyze the structure of phase space in our simplified system, *i.e.*, in the ERTBP, we computed FLI maps in the planar (2D) circular and elliptical cases. In the circular limit a direct comparison with surfaces of section (in the Hill limit, $\mu' \ll 1$, Astakhov & Farrelly 2004) can be made. We have previously demonstrated that in the planar CRTBP the FLI reproduces correctly all relevant features visible in the SOS (Astakhov & Farrelly 2004). In particular, the chaotic layer, as it evolves with increasing energy, can be easily identified by high values of the FLI. Note also that FLI measurements make sense even for relatively short time integrations, and, even in 2D, are much more efficient than is the construction of SOS (Froeschlé et al. 2000; Pilat-Lohinger et al. 2003; Astakhov & Farrelly 2004).

In the planar limit of the ERTBP initial conditions were generated randomly within the Hill radius on the surface of section (see Fig. 2 caption) taking, initially, $f = \pi/2$. This guarantees that the ERTBP initial conditions reduce to those of CRTBP (Astakhov & Farrelly 2004). For a given μ' and e all ERTBP initial conditions are, therefore, generated with identical initial energies (Astakhov & Farrelly 2004).

A further issue in generating the FLI maps in Fig. 6 concerns the choice of initial energy. Because we are comparing different masses and ellipticities it is not possible to work at exactly the same energy in each case. This is because in the ERTBP the energies of the Lagrange points, for example, depend on ellipticity, mass and the instantaneous value of the true anomaly, f. That is, energy (or the Jacobi constant, Murray & Dermott 1999) is not conserved in the ERTBP. Thus, in order to make a fair comparison of the dynamics between these different cases we need to construct a criterion of comparability; in practice, we selected initial values of the Jacobi constant such that the sizes of

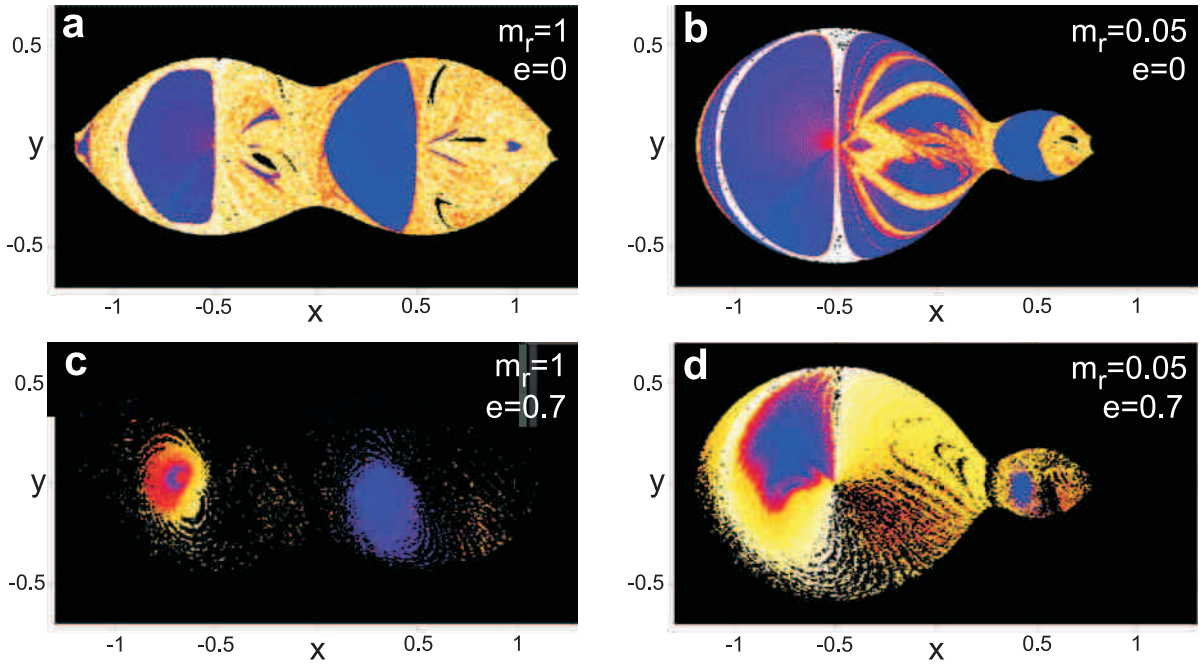

Figure 6. Fast Lyapunov indicator maps for the planar ERTBP and four eccentricity/mass ratio combinations. The origin is shifted so that the binary partners are located at $(x, y) = (\pm 0.5, 0)$ in scaled units and here units are rescaled so that $R_H = 1$. Colour scale runs from blue to red to white with increasing FLI. Initial energies are as defined in the text. Blank regions correspond to directly scattering or hyperbolic trajectories which survive for less than ~ 20 binary periods. Areas that resemble shotgun-like patterns of points correspond to chaotic regions (Astakhov & Farrelly 2004) (see the text). At the higher eccentricities scattering (hyperbolic) regions are noticeably larger for (c) (equal masses) than for (d) (unequal masses); this translates into enhanced capture probabilities for equal masses.

the gateways in the zero-velocity surface at time $t = 0$ (see Fig. 1) were comparable (Astakhov & Farrelly 2004). Approximately, this equates the fluxes of incoming/outgoing particles and facilitates a fair comparison of relative densities of chaotic versus hyperbolic orbits. The actual energies used at $t = 0$ ($f = \pi/2$) were $E = -1.725$ for $m_r = 1$ and $E = -1.675$ for $m_r = 0.05$. Admittedly this is an *ad hoc* approach but we find that the general appearance of the FLI plots is quite robust to the precise values of the initial Jacobi constant used provided that the gateways have similar sizes.

4.3.2 Interpretation of FLI maps

Figure 6 shows FLI maps for different mass ratios and eccentricities. It is easy to distinguish between chaotic regions, directly scattering (hyperbolic) regions and – to the intruder – inaccessible KAM regions (Astakhov & Farrelly 2004). In the chaotic regions nearby orbits tend to be dense and have similarly large FLI values. This results in chaotic regions having the appearance of a shotgun-like pattern – unlike in a SOS, however, each point corresponds to the initial condition of a *single* orbit coloured according to the final computed value of its FLI. By contrast, in hyperbolic regions orbits rapidly leave the Hill sphere and enter heliocentric orbits. We chose 20 mutual orbital periods of the primaries (in the ERTBP limit) as a cut-off such that orbits which survived for less than this cut-off were not plotted. We verified that our results are not sensitive to the precise choice of cut-off time. The large solid regions in Fig. 6 correspond to regular (KAM) regions. Elsewhere we have examined the effect of ellipticity on chaos-assisted capture and the differences in FLI maps for chaotic, hyperbolic and regular zones was examined in detail in the ERTBP (Astakhov & Farrelly 2004).

In summary, in FLI maps hyperbolic regions manifest themselves by their relative sparsity of points as compared to chaotic and regular zones (Astakhov & Farrelly 2004).

4.3.3 Effect of mass ratio and eccentricity on capture probabilities

First we compare the situation for equal versus unequal masses in the case of circular orbits, *i.e.*, Fig. 6a and 6b. Clearly the observable sea of chaos is much larger for frame (a) *i.e.,* equal masses, than for frame (b) *i.e.,* unequal masses. However, in both cases it is also true that there are relatively few hyperbolic regions. For the case of unequal masses the regular KAM regions are very large but since KAM regions represent barriers in phase space (Lichtenberg & Lieberman 1992) these regions are inaccessible to the intruder. Thus in both Fig. 6a and 6b an intruder is likely to become caught up in a chaotic zone thereby producing a resonance. According to our earlier arguments this will, on average, increase dwell-times and so tend to destabilize the binary. This suggests that circular (or very low eccentricity) binary orbits will be less likely to be captured.

Next we examine the case of higher eccentricity, $e = 0.7$, shown in Fig. 6c and 6d. This case is actually the most relevant to the real situation since the osculating eccentricity of the chaotic binary is generally quite high. For equal masses, shown in frame (c), very large hyperbolic regions

are clearly visible whereas in frame (d) (unequal masses) the "non-regular" regions are primarily chaotic rather than hyperbolic. Incoming intruders will therefore encounter very different environments between the two cases. If the binary partners are of equal mass, intruders will most likely enter hyperbolic regions and so will exit the Hill sphere promptly. In the case of unequal masses the battleground is of a very different nature, resembling a field of sticky mud in which intruders rapidly become bogged down. That is, they become temporarily trapped in trinary resonances which increases the probability that the binary will be disrupted rather than stabilized. This can be explained, in part, by noting that in the CRTBP with equal mass primaries (the Copenhagen problem, Szebehely 1967; Benet et al. 1997; Nagler 2004), the zero velocity surface is symmetric in x and so the gateways into and out of the capture region are equivalent. This facilitates quick transits through the capture zone, whereas in the asymmetric mass system one gateway is smaller than the other constituting a bottleneck which hinders passage.

The FLI maps in Fig. 6 provide a qualitative explanation of the observed mass effect. The dwell-times of intruders within the Hill sphere are a sensitive function of whether intruders enter hyperbolic or chaotic regions of phase space inside the Hill sphere. As system parameters change (total initial energy, ellipticity, etc.) the sizes and shapes of these regions alter in a highly nonlinear manner (see Fig. 2c) as is characteristic of chaotic scattering. With increasing ellipticity the sizes of the chaotic versus the directly scattering regions *decrease*, especially in the case of equal mass binary partners. This translates into enhanced capture probabilities for equal masses.

Overall, based on a comparison of the four cases in Fig. 6 in the ERTBP, we conclude that intruder stabilization will be most efficient for (i) equal masses and (ii) moderate to high eccentricity orbits. It is somewhat ironic that, in this mechanism, the existence of chaos in the binary orbit (produced by solar tides) is critical to nascent KBB formation, whereas if intruders enter zones of chaotic (as opposed to hyperbolic) scattering then the result is destabilization of the binary.

However, the ERTBP model has its limitations. The assumption that the mutual chaotic binary orbit can be treated (from the point of view of the intruder) as an elliptical Kepler orbit on short timescales is not valid if the actual binary orbit is itself extremely unstable on comparable timescales. Such three-body orbits tend to involve "near misses" of the binary partners and are less stable than are more "circular" three-body orbits (*e.g.,* see Fig. 2a). Thus for very high instantaneous eccentricities (orbital segments involving near misses) the binary partners (in the full four-body problem) are difficult to stabilize. This tends to reduce the capture probability into very high eccentricity orbits considerably.

The net effect of all of these considerations is to favor moderately elliptical binary mutual orbits when the binary partners have approximately equal masses. This is precisely what is found in our simulations and in actual observations of KBBs (Burns 2004; Noll et al. 2004a,b).

5 ALTERNATIVE FORMATION MODELS

Of the four paths mentioned in the Introduction and summarized in Table 1 extensive numerical simulations have only been reported for the exchange mechanism, Path 4 (Funato et al. 2004; Kolassa 2004). In this section we present a brief comparison of our multiple scattering model with alternative theories and also report some model simulations which we have performed for Paths 2 and 3 (Goldreich et al. 2002).

5.1 Exchange reactions

In the exchange reaction model (Funato et al. 2004) the first step is the formation of a binary through a two-body dissipative encounter. This can happen in two ways; (i) tidal disruption of an object during a close encounter followed by accretion of the resulting fragments to produce a binary; and, (ii) a "giant" impact in which coagulating debris after the collision produces a satellite orbiting a larger object. Main-belt asteroid binaries (and the Earth-Moon binary (Canup & Asphaug 2001; Canup 2004) and (with some important differences) possibly the Pluto-Charon binary (Canup 2005)) are thought to have formed in this manner. Generally, the result is a binary with an extreme mass ratio and a tight, circular orbit. In the exchange reaction mechanism, the mass ratio of such proto-binaries in the KB is increased through later gravitational scattering encounters with a third object originating (in the simulations) at infinity. Funato et al. (2004) modelled this by performing extensive scattering simulations between strongly asymmetric-mass binaries already following bound, compact, circular orbits and large incoming intruder masses. They found a propensity for the smaller member of the initial binary to be replaced by the intruder with the final binary then following a large, highly eccentric Keplerian orbit.

While this mechanism is plausible and does produce binaries which are at least qualitatively similar to known KBB orbits a number of difficulties nevertheless remain. In the first place, this mechanism does not provide an *ab initio* explanation for why the the mass ratios of actual KBBs are of order unity. Instead, it simply provides a route by which a binary can increase its mass ratio. Because Funato et al. assumed that the primary member of the initial binary and the intruder had equal masses then, if exchange occurs, a binary of order unity mass ratio is guaranteed to result. There appears to be no compelling reason, at least based on the simulations reported (Funato et al. 2004), to conclude that mass ratios of order unity should necessarily result from this process, only that exchange reactions can increase mass ratios.

In addition, exchange reactions seem to produce orbital eccentricities (and semimajor axes) larger than those typically observed (Noll 2003; Noll et al. 2004b). However, this might simply be the result of the particular choice of masses made by Funato et al. (2004). Thus it would be interesting to extend these simulations to include a broader range of intruder masses so as to understand (a) the role of intruder mass in determining the probability of exchange and (b) the effect of intruder mass on post-exchange orbital properties of the binary.

5.2 Two-body collisions inside the Hill sphere

The first mechanism proposed for the production of transneptunian binaries is that of Weidenschilling (2002). In this model two bodies accrete after a mutual collision within the Hill sphere of a third, larger, body. They then remain bound as a single object orbiting the larger body, thereby producing a binary. The main objections to this model have to do with the scarcity of large objects in the primordial KB. However, Petit & Mousis (2004) (see also Stern 2002) discuss this issue at length and conclude that the mechanism of Weidenschilling (2002) might have operated, possibly in tandem with other mechanisms. In the absence of detailed simulations it remains an open question whether this mechanism can provide quantitative agreement with the observed properties of KBBs.

5.3 Capture through dynamical friction

This mechanism was originally proposed by Goldreich et al. (2002). Here we have shown that the dynamical basis for this model is chaos-assisted capture (Astakhov et al. 2003; Astakhov & Farrelly 2004). No detailed simulations of KBB formation or their orbital and compositional properties were presented by Goldreich et al. (2002). Because this mechanism proceeds from similar assumptions to the one we propose, we performed a limited number of simulations in which multiple intruder scattering as an energy loss mechanism was replaced by dynamical friction, modelled as simple velocity dependent dissipation (Murray & Dermott 1999; Astakhov et al. 2003). We find that, dynamical friction provides an efficient route to binary capture and Keplerization, producing final orbital elements similar to those in Fig. 4. However, it is not sensitive to the mass ratio of the initial quasi-bound binary. This is because the scaled Hill equations (1), even including dissipation, contain no parameters and so cannot depend on the masses of the binary partners. Thus, no mass effect is predicted. Of course, more sophisticated models of dynamical friction (Chandrasekhar 1943; Binney 1977; Goldreich et al. 2004; Just & Peñarrubia 2004) might conceivably reveal such a preference. In addition, dynamical friction has been ruled out on the basis of estimates of planetesimal mass distributions although this issue may be worth revisiting (Funato et al. 2004).

5.4 The L^3 mechanism

Again, this mechanism was originally proposed by Goldreich et al. (2002) and is the most similar to the one which we present here. Although no simulations of L^3 were made by Goldreich et al. (2002) a number of issues can be raised in regard to it; (a) in L^3, as originally proposed, roughly equal mass binaries result directly from the assumption that a transient binary undergoes a scattering encounter with a third body of comparable mass to the binary partners (which are assumed to be themselves of similar mass). That is, the preference for order unity mass ratios is an inescapable result of the foundational assumptions of the model; (b) unless multiple L^3 type encounters are being assumed, then hardening and Keplerization of the large transitory binary must occur in a single encounter which seems unlikely. To test this we have performed simulations exactly as for Fig. 4 except using a large intruder. The results are summarized in Fig. 7 and indicate that multiple large body encounters tend to disrupt the binary catastrophically. Further, examination of the actual orbital elements produced in these simulations confirms that neither a single nor a small number of L^3-type events is usually sufficient to produce Keplerian orbits. Instead, after a small number of such encounters the orbits resemble those of the initial quasi-bound binary, *e.g.*, that shown in Fig. 2. In these cases Keplerian orbital elements cannot meaningfully be defined.

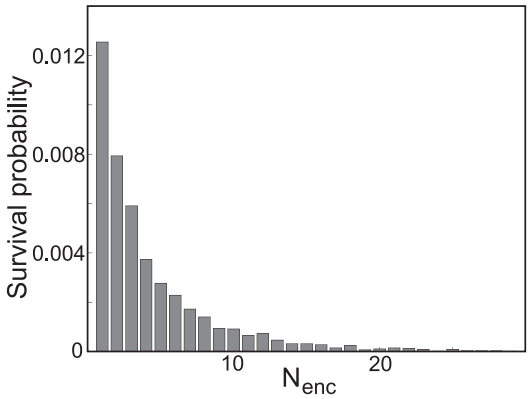

Figure 7. Histogram showing the survival probability of equal mass chaotic binaries ($\alpha_1 = \alpha_2$) after N_{enc} L^3 encounters with large intruders ($\alpha_3 = 0.3$, see equation (5)). 1000 initial binaries were taken with initial conditions for three-body Hill orbits and intruders originated as described in Sec. 3. To generate statistics the simulation was repeated 50 times, each time choosing the phase of each binary randomly with respect to the intruder.

Of course a hybrid of our model and L^3 is also possible. Certainly our simulations do not rule out the possibility of L^3-type collisions with additional hardening being produced through collisions with smaller bodies; however, L^3 collisions are not necessary for capture or to produce roughly equal mass binaries.

6 CONCLUSIONS

We have presented what are, to our knowledge, the first simulations of binary-intruder scattering in which the binary orbit is itself chaotic. Previous simulations of binary star intruder scattering have focussed on the important but simpler case in which the initial binary already follows a bound Keplerian ellipse. Here the binary orbits used are long living chaotic orbits (in the Hill approximation) which cling for long periods to regular KAM structures in phase space. These transitory orbits are possible only if the Sun-binary Hill sphere is taken into account. The importance of the Hill sphere in temporarily capturing Kuiper-belt binaries was first noted by Goldreich et al. (2002) on empirical grounds. The dynamical explanation for the results proposed here is chaos-assisted capture (Astakhov et al. 2003; Astakhov & Farrelly 2004; Holman et al. 2004).

Once a proto-binary has formed within the Hill sphere then, if it is to survive, some stabilization mechanism must operate. Our simulations demonstrated that multiple low-mass intruder scattering can not only stabilize transitory binaries but also provides an efficient route to binary hard-

ening and Keplerization of the orbit. By adjusting a single parameter – the number of intruder-binary encounters – we were able to obtain excellent agreement with the orbital properties of known KBBs. In particular, our simulations predict that KBBs will have moderate eccentricities. This is in good agreement with recent observations (Noll 2003; Noll et al. 2004a,b) and contrasts with the exchange mechanism of KBB formation which produces exclusively large eccentricities (Funato et al. 2004; Kolassa 2004).

Our simulations also lead to a striking preference for the production of binaries having roughly equal masses. Strongly asymmetric mass ratios – typical of main belt asteroid binaries – are selected against, and, again this appears to be consistent with observations. The model we propose is not set up to produce only order unity mass ratio binaries; nevertheless, a preference for mass ratios of order unity emerges.

An important difference between our model and L^3 concerns how the binary hardens. Single encounters with large intruders are unlikely to produce the relatively compact (as compared to R_H) Keplerian binary orbits that are actually observed. Moreover, we find that multiple encounters with large intruders tend, on average, to disrupt the binary. Instead, the model we propose involves a sequence of low-mass intruder events rather than a single scattering encounter with a massive object. It turns out that this provides an efficient mechanism for binary hardening and Keplerization. However, because we are unable to estimate the probabilities for the initial rate of production of quasi-bound binaries of varying mass ratios in the Hill sphere, it is unclear how strongly this mass effect will persist. Nevertheless, our simulations demonstrated that equal mass binaries have a much higher survival probability after multiple encounters than do asymmetrical mass ratio objects. Thus, we are confident that the mass effect we have found will not be washed out by the statistics of transitory binary formation.

Throughout we have assumed that the binary centre-of-mass follows a circular (heliocentric) orbit. However, in principle, we also need to consider the effect of introducing eccentricity into the heliocentric binary orbits. This is because some observed KBBs have significantly eccentric heliocentric orbits with perihelia close to, or even inside, Neptune's orbit (*e.g.,* Pluto-Charon, (47171) 1999 TC_{36} and (26308) 1998 SM_{165}). Typical KBB heliocentric ellipticities lie in the range $\sim 0.03 - 0.37$ (Noll 2003). In our recent study of capture and escape in the elliptic restricted three-body problem (Astakhov & Farrelly 2004) we found that the introduction of moderate heliocentric ellipticity reduces, but does not entirely eliminate, the efficacy of the chaos-assisted capture mechanism. While further study of this issue is clearly warranted, we expect that the results presented here will similarly carry over to the elliptic heliocentric case.

Of course, it is also possible that observed heliocentric TNO binary eccentricities are not primordial. Actually, this is suggested by the observation that massive bodies in eccentric orbits will tend to have large approach velocities apart from coincidences such as, *e.g.*, when perihelia are aligned. Because such cases are rare, relative velocities will tend to be large and this will serve to reduce the probability of capture into chaotic orbits. This conclusion is consistent with results for capture in the elliptic restricted three-body problem (Astakhov & Farrelly 2004). These considerations suggest that, as with Paths 1 - 3, binaries formed when the disk was massive and dynamically cold, *i.e.,* prior to the dynamical excitation and depletion of the Kuiper-belt (Duncan & Levison 1997; Gomes 2003; Morbidelli et al. 2004).

Finally, we note that Figs. 3-5 demonstrate that, while significant, the selection for order unity mass ratio objects is not to the complete exclusion of smaller mass ratios. For example, the differences in dwell-time distributions are not so great as to eliminate the capture of small mass-ratio binaries entirely. Rather, Figs. 3 and 4 lead us to predict that a sizeable population of asymmetric mass KBBs is probably awaiting detection. Heralds of this group of objects might already exist in the low mass ratio binary objects (47171) 1999 TC_{36} (Trujillo & Brown 2002; Altenhoff et al. 2004) and (26308) 1998 SM_{165} (Brown & Trujillo 2002; Stern 2002; Noll 2003; Petit & Mousis 2004).

ACKNOWLEDGMENTS

This work was supported by grants from the US National Science Foundation through grant 0202185 and the Petroleum Research Fund administered by the American Chemical Society. All opinions expressed in this article are those of the authors and do not necessarily reflect those of the National Science Foundation. S. A. A. also acknowledges support from Forschungszentrum Jülich. We thank Kevin Hestir for valuable suggestions and comments on the manuscript. We also thank two anonymous referees for helpful and insightful suggestions.

REFERENCES

Aarseth S. J., 2003, Gravitational N-body Simulations: Tools and Algorithms. Cambridge Univ. Press, Cambridge
Altenhoff W. J., Bertoldi F., Menten K.M., 2004, A&A, 415, 771
Astakhov S. A., Burbanks A. D., Wiggins S., Farrelly D., 2003, Nat, 423, 264
Astakhov S. A., Farrelly D., 2004, MNRAS, 354, 971
Benet L., Trautmann D., Seligman T. H., 1997, Celest. Mech. Dynam. Astron., 66, 203
Bernstein G. M., Trilling D. E., Allen R. L., Brown M. E., Holman M., Malhotra R., 2004, AJ, 128, 1364
Binney J., 1977, MNRAS, 181, 735
Boyd P. T., McMillan S. L. W. 1993, Chaos, 3, 507
Brasser R., 2002, MNRAS, 332, 723
Brown M. E., Trujillo C. A., 2002, IAU Circular 7807.
Burns J. A., 2004, Nat, 427, 494
Canup R. M., Asphaug, E., 2001, Nat, 412, 708
Canup R. M., 2004, Icarus, 168, 433
Canup R. M., 2005, Sci, 307, 546
Chandrasekhar S., 1943, ApJ, 97, 255.
Chauvineau B., Farinella P., Harris A. W., 1995, Icarus, 115, 36
Christy J. W., Harrington R. S., 1978, AJ, 83, 1005
Duncan M. J., Levison H. F., 1997, Sci, 276, 1670
Durda D. D., 2002, Nat, 420, 618

Durda D. D., Bottke W. F., Enke B. L., Merline W. J., Asphaug E., Richardson D. C., Leinhardt Z. M., 2005, Icarus, 167, 382
Elliot J. L. et al., 2005, AJ, 129, 1117
Eddington A. S., 1924, MNRAS, 84, 308.
Froeschlé C., Guzzo M., Lega E., 2000, Sci, 289, 2108
Funato Y., Makino J., Hut P., Kokubo E., Kinoshita D., 2004, Nat, 427, 518
Gladman B., 2005, Sci, 307, 71
Goldreich P., Ward W. R., 1973, ApJ, 183, 1051
Goldreich P., Lithwick Y., Sari R., 2002, Nat, 420, 643
Goldreich P., Lithwick Y., Sari R., 2004, ARA&A, 42, 549
Gomes R. S., 2003, Icarus, 161, 404
Heggie D. C., 1975, MNRAS, 173, 729
Heggie D., Hut P., 2003, The gravitational million-body problem, Cambridge Univ. Press, Cambridge
Hénon M., Petit J.-M., 1986, Celest. Mech., 38, 67
Hills J. G., 1975, AJ, 80, 809
Hills J. G., 1983a, AJ, 88, 1269
Hills J. G., 1983b, AJ, 88, 1857
Hills J. G., 1990, AJ, 99, 979
Hut P., Bahcall J. N., 1983, ApJ, 268, 319
Holman M. J. et al., 2004, Nat, 430, 865
Inagaki S., 1984, MNRAS, 206, 149
Janes K., ed., 1991, The Formation and Evolution of Star Clusters, ASP Conf. Ser., 13, Astron. Soc. Pac., San Francisco, CA.
Just A., Peñarrubia J., 2004, A&A, preprint (astro-ph/0410740)
Karplus M., Porter R. N., 1970, Atoms & Molecules, Benjamin Cummins, Menlo Park, CA. pp. 454-458
Kenyon S. J., Bromley B. C., 2004, AJ, 128, 1916
Kolassa S., 2004, (preprint at http://www.minet.uni-jena.de/preprints/kolassa_04/kuiper_centaurs.pdf)
Lewis M. C., Stewart, G. R., 2002, Icarus, 153, 224
Lichtenberg A. J., Lieberman M. A., 1992, Regular and Chaotic Dynamics, 2nd edn. Springer-Verlag, NY
Llibre J., Piñol J., 1990, Celest. Mech. Dynam. Astron., 48, 319
Luu J. X., Jewitt D. C., 2002, ARA&A, 40, 63
Macau E. E. N., Caldas I. L., 2002, Phys. Rev. E, 65, 026215
Mardling R. A., 1995a, ApJ, 450, 722
Mardling R. A., 1995b, ApJ, 450, 732
Margot J. L., 2002, Nat, 416, 694
Merline W. J., Weidenschilling S. J., Durda D. D., Margot J-L., Pravec P., Storrs A., 2003, in Bottke W. F., Cellino A., Paolicchi P., Binzel R. P., ed., Asteroids III. Univ. Arizona Press, Tucson, 289
Mikkola S., Valtonen M. J., 1992, MNRAS, 259, 115
Morbidelli A., Emel'yanenko V. V., Levison H. F., 2004, MNRAS, 355, 935
Murray C. D., Dermott S. F., 1999, Solar System Dynamics. Cambridge Univ. Press, Cambridge
Nagler J., 2004, Phys. Rev. E, 69, 066218
Nazzario R. C., Hyde T. W., 2005, CASPER-05-02 report, preprint (physics/0501113)
Noll K. S., 2003, Earth, Moon & Planets, 92, 395
Noll K. S., Stephens D. C., Grundy W. M., Griffin I., 2004a, Icarus, 172, 402
Noll K. S., Stephens D. C., Grundy W. M., Osip D. J., Griffin I., 2004b, AJ, 128, 2547
Ohtsuki K., Stewart G. R., Ida S., 2002, Icarus, 155, 436
Osip D. J., Kern S. D., Elliot J. L., 2003, Earth, Moon & Planets, 92, 409
Petit J.-M., Mousis O., 2004, Icarus, 168, 409
Pilat-Lohinger E., Funk B., Dvorak R., 2003, A&A, 400, 1085
Press W. H., Teukolsky S. A., Vetterling W. T., Flannery B. P., 1999, Numerical Recipes in C, 2nd edn. Cambridge Univ. Press, Cambridge
Quinlan G. D., 1996, New Astron., 1, 35.
Rafikov R. R., 2003, AJ, 125, 942
Schaller E. L., Brown M. E., 2003, BAAS, 35, DPS 35th Meeting, abstr. No. 39.20
Scheeres D. J., 1998, Celest. Mech. Dynam. Astron., 70, 75
Scheeres D. J., Bellerose J., 2005, Dynam. Syst., 20, 23
Shebalin J. V., Tippens A. L., 1996, A&A, 309, 459
Simó C., Stuchi T. J., 2000, Physica D, 140, 1
Stern S. A., 2002, AJ, 124, 2300
Stewart G. R., 1997, Nat, 387, 658
Stewart G. R., Ida S. 2000, Icarus, 143, 28
Stiefel E. L., Scheifele G., 1971, Linear and Regular Celestial Mechanics: Perturbed Two-Body Motion, Numerical Methods, Canonical Theory. Springer-Verlag, New York
Szebehely V., 1967, Theory of Orbits: the Restricted Problem of Three Bodies. Acad. Press, NY and London
Takahashi S., Ip W. H., 2004, PASJ, 56, 1099
Tancredi G., Sánchez A., Roig F., 2001, AJ, 121, 1171
Toth I., 1999, Icarus, 141, 420
Trimble V., Aschwanden M. J., 2003, PASP, 116, 187
Trujillo C. A., Brown M. E., 2002, IAU Circular 7787
Veillet C. et al., 2002, Nat, 416, 711
Weidenschilling S. J., 2002, Icarus, 160, 212
Wetherhill G. W., Stewart G. R., 1993, Icarus, 106, 190
Xu S., Binzel R. P., Burbine T. H., Bus S. J., 1995, Icarus, 115, 1
Zaslavsky G. M., 1985, Chaos in Dynamic Systems, Harwood Academic Publ., NY